European Journal of Chemistry

Synthesis and microstructure studies of nano-sized cerium phosphates

Adly Abdella Hanna[a], Sahar Mohamed Mousa[a], Gehan Mahmoud Elkomy[b] and Marwa Adel Sherief[a,*]

[a] *Inorganic Chemistry Department, National Research Centre, Dokki, Cairo, 11787, Egypt*
[b] *Electron Microscopes and Thin Film Department, National Research Centre, Dokki, Cairo, 11787, Egypt*

Corresponding author at: Inorganic Chemistry Department, National Research Centre, Dokki, Cairo, 11787, Egypt. Tel.: +20.10.5249230; fax: +20.2.33335968.
E-mail address: gohamora@yahoo.com (M.A. Sherief).

ARTICLE INFORMATION

ABSTRACT

Cerium phosphate, $CePO_4$, nanoparticles with hexagonal or monoclinic phase was synthesized by the reaction between $Ce(SO_4)_2.4H_2O$ and two different phosphate sources, H_3PO_4 and Na_2HPO_4. The obtained gel was dried and calcined at different temperatures (200, 400, and 800 ℃). The effects of the precursor materials and the calcination temperatures on the produced phases were studied. Both X-ray diffraction (XRD) and infrared spectroscopy (IR) were used to follow the changes in the phase structure for the produced samples. The thermal behaviour of the as prepared samples was studied by using differential scanning calorimetric (DSC) and thermogravimetric analysis (TGA). The morphology, crystallinity and particle size of the produced samples as prepared and calcined were characterized by transmission electron microscope (TEM). The analysis of TEM results indicated that $CePO_4$ was prepared in nano-sized particles.

1. Introduction

Since the discovery of the crystalline layered structure of the tetravalent cations by Clearfield *et al.* [1] and Alberti *et al.* [2], several modifications were carried out to enhance the application of their phosphates in different fields. During the last decade, our attention was paid to synthesis, characterization and applications of the rare earth phosphates because they have different uses in the field of technology such as cation exchange, intercalation, proton conductivity, *etc*.

In previous works, the authors studied the preparation, characterization and applications of some simple and condensed phosphates including Na, Al, Fe, Ti and Zr and some rare earth phosphates [3,4]. Both the classical and the advanced methods were used in the preparation and the produced phosphates were evaluated as ion exchangers for removing the small and the large cations from their aqueous medium. Other phosphates were used as humidity sensors depending on the improvement of their semiconducting properties by substituting the tetravalent cations by mono- and divalent cations [5]. According to this research policy our interest was paid to prepare $CePO_4$ for using in different applications at high temperature because it is thermally stable with a melting point at $\sim$ 2000 ℃ [6].

The forgoing of the literatures survey indicates that the cerium phosphates can be used in different industrial and environmental applications such as a potential storage material for nuclear waste [7], a poison to automobile catalyst [8-12], and potential proton conduction membrane for the hydrogen fuel cell [13]. More recently, some studies were done to introduce cerium phosphate in the optical field [14,15]. The optical reflection spectrum of $CePO_4$ is affected critically by their crystallization which by turn depends on the method of preparation as well as the calcination temperature [16-17]. On the other hand, the optical properties depend quietly on the thermal properties of the cerium phosphates. Therefore, this work was devoted to prepare cerium phosphate by using different precursor materials to study their effects on the produced phosphates. Moreover, the effect of the calcinations temperature on the produced phases by using X-ray diffraction, IR spectra, thermal analysis (DSC/TG) and TEM was studied to follow the changes in the phase structure and the crystallinity by heat treatment and processing technique.

2. Experimental

2.1. Procedure

For preparing the cerium phosphates, two methods were used depending on different sources of phosphates. The first method (I) was based on the chemical reaction between phosphoric acid and $Ce(SO_4)_2.4H_2O$, and using ammonia solution for precipitation. By adding the stoichiometric amount of H_3PO_4 (0.84 mL) dropwise to $Ce(SO_4)_2.4H_2O$ (5 g) (P/Ce=1) mole ratio with continuous stirring, a gel solution was obtained. This gel was converted to a suspension state by adding ammonia dropwisly, where the pH of the final reaction became 8 and kept for 24 hr at room temperature. The formed solid was separated by filtration through a centrifuge and dried at 100 ℃. The second method of preparation (II) depends on mixing stochiometric solutions of disodium hydrogen phosphate $Na_2HPO_4.2H_2O$ (1.93 g) and $Ce(SO_4)_2.4H_2O$ (5 g) with continuous stirring, and the pH of final reaction is 4. The formed gel were maintained for 24 hr at 75 ℃ and then separated and dried at 100 ℃. To study the effects of the calcination temperatures on the formed phases, both samples (I) and (II) were calcined at different temperatures, namely 200, 400 and 800 ℃.

2.2. Characterization

The produced samples were characterized by X-ray diffraction to study the phase transition. The diffraction patterns were obtained by means of a chart recording Brukur D8 advanced X-ray diffractometer using copper (K_α) radiation. Infrared measurements (IR) were recorded by JASCO-FT/CR-3000E infrared spectrophotometer from 4000 to 400 cm^{-1} and the thermal analysis was performed by USA Perkin-Elmer thermogravimetric up to 1000 °C with heating rate 10 ° C/min. The morphology and the crystallinity of the prepared samples before and after calcination were examined by transmission electron microscope (TEM) Joel JEM 1230 working at 100 keV. Also Gatan program was used to calculate the d-spacing from the selected area electron diffraction SAED patterns.

3. Results and Discussion

The X-ray diffraction patterns of the as prepared samples with that thermally treated at different temperatures 200, 400 and 800 °C were shown in Figure 1a by using method (I) and Figure 1b for using method (II). The X-ray patterns show that both the as prepared samples and those heated at 200 °C are amorphous independent on precursor materials, whatever it is phosphoric acid or di-sodium hydrogen phosphate. This finding is in agreement with other works using different routes for preparation such as the hydrothermal method [18], or the mechanochemical method [19]. By heating the produced samples to 400 °C for 2 hr, only one phase of $CePO_4$ (Monazite) was formed by using method (I) according to the card no. [83-0652] while two different phases of cerium phosphates (Monazite) $CePO_4$ and pyrophosphate (orthorhombic) CeP_2O_7 were formed by using method (II). By raising the calcination temperature of this sample to 800 °C, the pyrophosphate was converted to orthophosphate (rhabdophane with hexagonal crystal structure) as shown in Figure 1b. The presence of two different phases may be explained by the formation of an intermediate compound at the first stage of preparation and has the chemical composition $Ce_{1-x/3}(PO_4)_{1-x}(HPO_4)_x \cdot nH_2O$ where the phosphate source for this sample was Na_2HPO_4, so the presence of HPO_4^{2-} species can be found and reacted easily with Ce^{3+} leading to the formation of previous chemical composition. By calcination, this compound was decomposed to $CePO_4$ and CeP_2O_7 with water evaporation [20]. The X-ray results are in agreement with the results obtained by Masui *et al.* [21], where they observed that the preparation of $CePO_4$ gives an amorphous state up to 723 K and above this temperature other phases were observed as $CePO_4$ and CeP_2O_7 where CeP_2O_7 is converted to $CePO_4$ by calcination above 1173 K. It may be concluded that the produced phases of $CePO_4$ are greatly dependant on the methods of preparation and the precursor materials (the phosphates species in the medium) as reported from the previous work [22-24] who used $Ce(SO_4) \cdot 4H_2O$ for preparation. It seems that, the resulting $CePO_4$ is trivalent cations while it was added in the tetravalent state, this may be due to the reduction of Ce^{4+} to Ce^{3+} in the acidic medium. This behaviour is explained by the fact that the energy of the inner 4f level of the cerium is nearly the same as that of the outer valence electrons, and only small energy is required to change this state and hence the Ce^{4+} is easily converted to Ce^{3+} in the acidic medium [25].

To confirm these results, two samples of the final products were exposed to chemical analysis by using the Inductively Coupled Plasma-Atomic emission spectrometry (ICP-AES) technique. The first sample was prepared by method (I) and calcinated at 400 °C for 2hr, and the second was prepared by method (II) and calcinated at 400 °C. The results of analysis show that the mole ratio of Ce/P = 1.40 and 1.43 for the samples (I) and (II) respectively. The experimental results are

in agreement with the theoretical values of Ce/P which equals to 1.4 with negligible deviation.
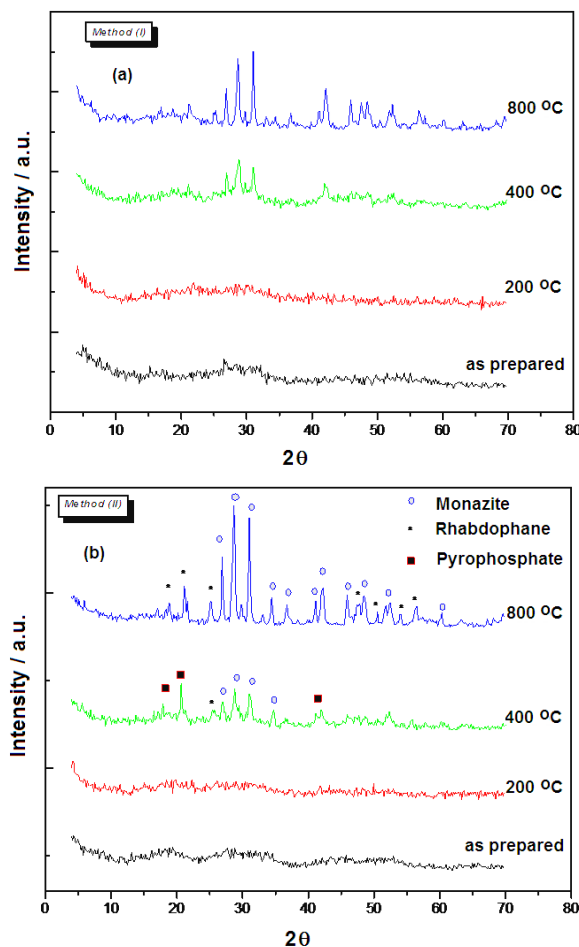

Figure 1. X-ray diffraction patterns of the as prepared sample with that thermally treated at the temperatures of 200, 400and 800 °C; (a) using method (I) and (b) using method (II).

The IR spectrum of the as prepared samples by the two previous methods (I) and (II) as well as the calcined samples are recorded in Figure 2a and b. For the as prepared samples, the IR spectra behave nearly the same trend independent on the method of preparation. The IR charts show the appearance of an absorption bands at 3898-3209 cm^{-1} due to OH stretch and another peak at ~1632 cm^{-1} which is attributed to OH bending mode [26]. The absorption band characterizing the general phosphates band is pointed at 1430 cm^{-1} [27]. A series of absorption bands are characterized at 1066, 619 and 520 cm^{-1} corresponding to P-O stretching, O=P-O bending and O-P-O bending mode vibration respectively. The appearances of these bands are typical for the hydrous $CePO_4$ as suggested by Hazel et al [28]. For the synthesized materials calcined at 200 °C, the IR spectra showed three distinct bands for hydrous hexagonal orthophosphates at 1053, 619 and 544 cm^{-1} for the sample prepared by method (I), while only two bands occurred for the sample prepared by method (II) at 599 and 528 cm^{-1}, while the third band was shifted to 1070 cm^{-1} due to the symmetric stretching of terminal group from pyrophosphate [22]. The IR spectra of the samples prepared using method (I) reveals an additional band occurred at 431 cm^{-1} due to PO_4^{3-} vibration [29]. For the calcined samples at 400 °C, the IR charts have the same behavior as shown previously with the appearance of some additional bands. These new bands appeared at 440-420 cm^{-1} due to the PO_4^{3-} vibration for both methods (I) and (II) but the other one which appeared at 943

cm^{-1} corresponding to the crystallization of the pyrophosphate is only observed for method (I) [30]. The IR spectra of the samples calcined at 800 ^{o}C reveals a band splitting for the wave number ranges 1100-950 cm^{-1} and 600-500 cm^{-1}. Occurrence of several bands in this region is characteristic for the vibration of PO_4^{3-} group in the lanthanide phosphates of monoclinic symmetry (Monazite structure) and agrees well with the literature data [28]. At 480-435 cm^{-1} some bands were appeared for the all samples prepared by the two methods due to PO_4^{3-} vibration.
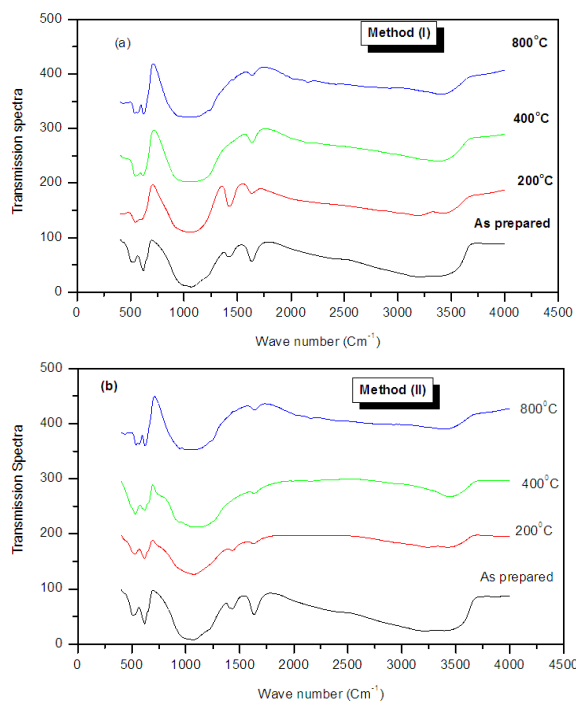

Figure 2. IR transmission spectra of the as prepared sample with that thermally treated at the temperatures of 200, 400and 800 ^{o}C; (a) using method (I) and (b) using method (II).

TG/DSC curves of the as prepared samples by using method (I) and dried at ~100 ^{o}C are represented in Figure 3a. The obtained curves show several weight loss regions. The first one occurred at ~100 ^{o}C and is attributed to the loss of the physosorbed water and it is confirmed by appearance of an endothermic peak at ~100 ^{o}C. The second stage recorded at ~250 ^{o}C is due to the loss of water of hydration as confirmed by the presence of small endothermic peak on the DSC curve [31]. This stage is corresponding to the conversion of the hydrated cerium phosphates, hexagonal rhabdophane to dehydrated phosphate according to the following equation [24], $CePO_4.nH_2O \Leftrightarrow CePO_4 + nH_2O$.

The third weight loss stage observed at ~330 ^{o}C and attributed to the transformation of $CePO_4$ from the amorphous state to the crystalline form and emphasized by an exothermic peak at the same region. The last weight loss stage occurred at ~450 ^{o}C is due to a complete crystallization which confirmed by the presence of small exothermic peak at ~450 ^{o}C.

The appearance of an exothermic peak on the DSC curve at ~600 ^{o}C may due to the conversion of hexagonal phase of $CePO_4$ to monoclinic structure as indicated by the following equation [24]: $CePO_4$ (Hexagonal) $\Leftrightarrow CePO_4$ (Monoclinic).

For the TG/DSC curves of the synthesized samples which prepared using method (II) as shown in Figure 3b, several sequence weight loss steps were occurred. The first step at around 114 ^{o}C and is attributed to the loss of physosorbed water with an endothermic peak at the same region and identical to the sample prepared by method (I). The second and

the third steps were confirmed by the presence of broad exothermic peak occurred at 250 ^{o}C to 350 ^{o}C and may be attributed to the loss of water and oxygen forming pyrophosphate structure (CeP_2O_7) and anhydrous hexagonal rhabdophane ($CePO_4$) [32]. The appearance of broad exothermic peak which started at around 400°C and ended at ~550 ^{o}C emphasizes the transformation of both amorphous (CeP_2O_7) and ($CePO_4$) phases to their crystalline structure. The last weight loss step occurred at nearly 630 ^{o}C may be attributed to the conversion of pyrophosphate to orthophosphate structure with the evolving of oxygen gas [33]. The appearance of an exothermic peak at around ~700 ^{o}C is due to the conversion of anhydrous hexagonal form of $CePO_4$ to monoclinic structure [33]. The thermal analysis results confirmed that the formation of an intermediate compound $Ce_{1-x/3}(PO_4)_{1-x}(HPO_4)_x.nH_2O$ in method (II) is responsible for the presence of different phases.
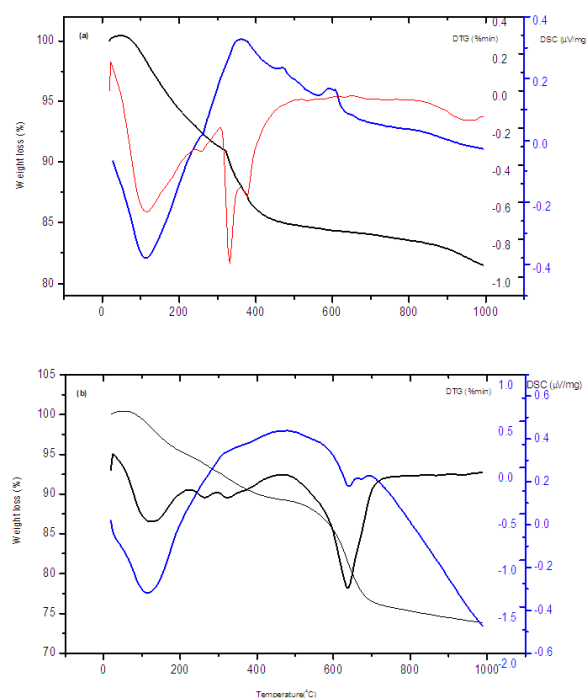

Figure 3. TG/DSC curves of the as prepared sample (a) using method (I) and (b) using method (II).

Further insight into the morphology and the microstructure of the produced samples in nanostructure was gained using transmission electron microscope (TEM) and selected area electron diffraction pattern (SAED). Figure 4 and 5 represent a set of micrographs and their corresponding SAED patterns. For the samples synthesized with methods (I) and (II) and calcined at different temperatures. The structure of as prepared samples produced by both methods (I) and (II) is appeared as amorphous states with no distinct microstructure Figure 4a and 5a. This can be clearly observed from the corresponding SAED in the inset of both figures. For the sample calcined at 200 ^{o}C, TEM micrograph Figure 4b shows that the product composed of a self-assembling of very fine particles forming a uniform nanostructure. This assembling is in a sphere like morphology with a size up to 52 nm. The corresponding SAED in the inset of Figure 4b reveals very week crystallinity of the product [which couldn't be detected from X-ray diffraction pattern]. Figure 4b-d shows that, increasing the heat treatment temperatures from 200 ^{o}C to 800 ^{o}C, gradually improves the crystallinity nature of the prepared nanoparticles of the produced samples. This finding is in agreement with the statement previously suggested [18]. At 400 ^{o}C, Figure 4c, the

Table 1. Summary of the physical properties of samples prepared by method (I) at different calcination temperatures as determined by X-ray and TEM.

Samples	Crystal structure	Morphology	Particle size (nm)
As prepared	-	Amorphous	-
Calcinated at 200 ºC	-	Spherical particles	52 nm diameter
Calcinated at 400 ºC	Monoclinic	Spherical particles	7-9 nm diameter
Calcinated at 800 ºC	Monoclinic	Spherical particles	18 nm diameter

Table 2. Summary of the physical properties of samples prepared by method (II) at different calcination temperatures as determined by X-ray and TEM.

| Samples	Crystal structure	Morphology	Particle size (nm)
As prepared	-	Amorphous	-
Calcinated at 200 ℃	Hexagonal-orthorhombic	Rod-shaped and spherical particles	24 nm diameter*60 nm length; 52 nm diameter
Calcinated at 400 ℃	Orthorhombic	Spherical particles	58-60 nm length
Calcinated at 800 ℃	Hexagonal – monoclinic	Needle shaped and Spherical particles	20 nm diameter

self assembling of particles preferred to disperse into nanoparticles with monoclinic structure which related to $CePO_4$ (Monazite phase) as confirmed previously from X-ray diffraction results. The crystal size is in the range from 7-9 nm, and the particle size decreased with raising calcination temperature due to dispersing the assembling [28] as observed in the thermal analysis investigation. A polycrystalline structure of very fine particle distribution can be seen from the corresponding SAED pattern.

(a)

(b)

(c)

(d)
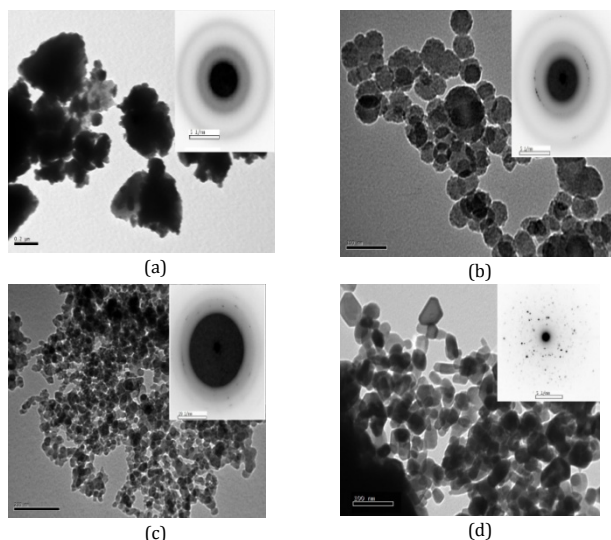
Figure 4. TEM micrographs and corresponding SAED patterns of cerium phosphate prepared using first method (I) at different calcinations temperature; (a) as prepared, (b) 200 ℃, (c) 400 ℃ and (d) 800 ℃.

At 800 ℃ Figure 4d, the TEM micrograph shows a complete crystallization of monoclinic structure ($CePO_4$) and a slight increase in the particle size (15-19 nm) (Table 1 and 2). The corresponding SAED pattern indicates that the formed phase is purely $CePO_4$ in monazite structure and there is no other phases appeared as confirmed previously from X-ray analysis.

In case of using method (II), the morphology of the sample calcined at 200 ℃, Figure 5b and 5c, contains two different phases, rode and sphere like shaped particles. The corresponding SAED pattern showed that the two phases are due to the formation of CeP_2O_7 and $CePO_4$ respectively. Raising calcination temperature to 400 ℃, the nanoparticles tend to have a high preferred orientation and the rod shaped particles disappeared and the spheres like- shaped particles were only found as shown from Figure 5d. At 800 ℃, the morphology consists of both monoclinic crystal structure and needle shaped particles due to the formation of monazite and rhabdophane respectively Figure 5e and 5f. This may be due to the conversion of CeP_2O_7 to the orthophosphate structure [33]. This calcinations temperature showed high crystallinity than the others as clearly seen from the corresponding SAED pattern in the inset of the previous figure.

The role of the precursors materials may explain by the statement which reported by Caswell and Jia *et al.* [34,35] for the controlling the shape of the nanoparticles by the inorganic species. For cerium phosphate, the excessive PO_4^{3-} anions might be responsible for the morphologies formation of the prepared nanostructure $CePO_4$. According to the crystal structures of the hexagonal and monoclinic $CePO_4$, it could be found that the Ce atoms in the two structures are surrounded by a different number of PO_4 tetrahedrons [36]. In the hexagonal $CePO_4$, the Ce atom connects six tetrahedral PO_4, while the Ce atom connects seven tetrahedral PO_4 in the monoclinic $CePO_4$. Obviously, to form monoclinic $CePO_4$, the Ce atom needs to be connected with more PO_4^{3-}; high PO_4^{3-} concentration might be beneficial for its crystallization. In the case of using H_3PO_4 as a source of PO_4^{3-} in the acidic medium, the solution is predominant with H_2PO_4 while at high pH (pH =8) the solution is predominant with PO_4^{3-} species which capable to form $CePO_4$. In the case of using Na_2HPO_4 as a source of the phosphates, the medium was rich with $NaHPO_4^-$ and HPO_4^{2-} so that the structure was strongly affected by the nature and the concentration of the phosphate species.

(a)

(b)

(c)

(d)

(e)

(f)
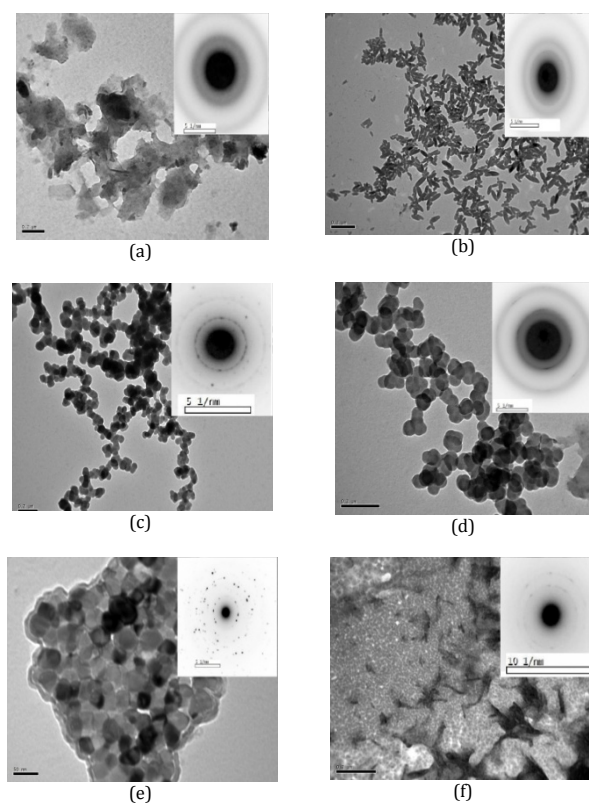
Figure 5. TEM micrographs and corresponding SAED patterns of Cerium phosphate prepared using second method (II) at different calcinations temperature; (a) as prepared, (b, c) 200 ℃, (d) 400 ℃ and (e, f) 800 ℃.

4. Conclusions

Both orthophosphates with hexagonal and monoclinic structures were prepared using the wet method by reacting $Ce(SO_4)_2.4H_2O$ with two different phosphate sources, namely H_3PO_4 & Na_2HPO_4. The X-ray results showed an amorphous state occurring for both as prepared and calcined samples at 200 ᵒC, independent on the phosphate source. A single phase of Monazite was formed by using H_3PO_4 but a mixture of Monazite and Rhapdophane structure were formed by using Na_2HPO_4. Both of IR spectra and thermal analysis results confirmed the X-ray results. Also, the morphology, crystallinity and the particle size of the produced samples were studied by TEM technique. The calculated particle size of the produced phosphate by using H_3PO_4 as a source of phosphate lies in the range of 12-19 nm and it is smaller than that obtained by using Na_2HPO_4 (20-60 nm). This may be due to the nature and the concentration of the phosphate species.

References

[1]. Clearfield, A.; Stynes J. A. *J. Inorg. Nucl. Chem.* **1964**, *26*, 117 -129.
[2]. Alberti, G.; Torracca, E. *J. Inorg. Nucl. Chem.* **1968**, *30*, 317 -318.
[3]. Hanna, A. A.; Ali, A. F.; Gad, A. E. *Phos. Res. Bull.* **2009**, *23*, 83 -89.
[4]. Khalil, M. Sh.; Hanna, A. A.; El-Sayed, M. A. *Phos. Res. Bull* **2002**, *14*, 77-88.
[5]. Hanna, A. A.; Mousa, S. M.; Ali A. F.; Sherief, M. A. *Phos. Res. Bull.* **2007**, *21*, 78-83.
[6]. Hikichi, Y., Nomura, T., Timura, Y.; Suzuki, S. *J. Am. Ceram. Soc.* **1990**, *73(12)*, 3594-3596.
[7]. Rappaz, M.; Abraham, M. M.; Ramey, J. O.; Boatner, L. A. *Phys. Rev. B* **1981**, *23(3)*, 1012-1030.
[8]. Xu, L.; Guo, G.; Uy, D.; Neill, A. E.O; Weber, W. H.; Rokosz, M. J.; McCabe, R. W. *Appl. Catal. B-Environ.* **2004**, *50*, 113-125.
[9]. Gee, B.; Horne, C. R.; Cairns, E. J.; Reimer, J. A. *J. Phys. Chem. B* **1998**, *102(50)*, 10142-10149.
[10]. Adler, S. B.; Reimer, J. A. *Solid State Ion.* **1996**, *91*, 175-181.
[11]. Duncan, M.; Chemical Shift Tensors, 2ⁿᵈ edition, Farragut Press, Madison, WI, **1997**.
[12]. Lopez Granados, M.; Cabello Galisteo, F.; Lambrou, P. S.; Mariscal, R.; Sanz, J.; Sobrados, I.; Fierro, J. L. G.; Efstathiou, A. M. *J. Catal.* **2006**, *239*, 410–421.
[13]. Kitamura, N.; Amezawa, K.; Tomii, Y.; Hanada, T.; Yamamoto, N.; Omata, T.; Otsuka-Yao-Matsuo, Y. *J. Electrochem. Soc.* **2005**, *152(4)*, A658-A663.
[14]. Mehta, V.; Aka, G.; Dawar, A. L.; Mansingh, A. *Opt. Mater.* **1999**, *12*, 53-63.
[15]. Imanaka, N.; Masui, T.; Hirai, H.; Adachi, G. *Chem. Mater.* **2003**, *15*, 2289-2291.
[16]. Onada, H.; Nariai, H.; Moriwaki, A.; Maki, H.; Motooka, I. *J. Mater. Chem.* **2002**, *12*, 1754-1760.
[17]. Feldmann, C.; Jungk, H. O. *J. Mater. Sci.* **2002**, *37*, 3251-3254.
[18]. Sato, T.; Sato, C.; Yin, S. *Phos. Res. Bull.* **2008**, *22*, 17-21.
[19]. Matraszek, A.; Szczygiel, I.; Macalik, L.; Hanuza, J. *J. Rare Earths* **2009**, *27(4)*, 598-602.
[20]. Penot, C.; Champion, E.; Goursat, P. *Phos. Res. Bull.* **1999**, *10*, 307-312.
[21]. Masui, T.; Hirai, H.; Imanaka, N.; Adachi, G. *J. Alloy and Comp.* **2006**, *408-412*, 1141-1144.
[22]. Masui, T.; Hirai, H.; Imanaka, N.; Adachi, G. *Phys. Status A* **2003**, *198(2)*, 364-368.
[23]. Lucas, S.; Champion, E.; Bernache-Assollant, D.; Leroy, G. *J. Solid State Chem.* **2004**, *177*, 1312-1320.
[24]. Lucas, S.; Champion, E.; Bregiroux, D.; Bernache-Assollant, D.; Audubert, F. *J. Solid State Chem.* **2004**, *177*, 1302-1311.
[25]. Pradyot Patnaik. Handbook of Inorganic Chemicals, McGraw-Hill, 2002.
[26]. Bo, L.; Liya, S.; Xiaozhen, L.; Shuiche, Z.; Yumeri, Z.; Tianmain, W.; Sasaki, Y.; Ishii, K.; Kashiwaya, Y.; Takahashi H.; Shibayama, T. *J. Mater. Sci. Lett.* **2001**, *20*, 1071-1075.
[27]. Khawaja, M. A.; Khahak, I. G. *J. Sci. Ind. Res.* **1994**, *37*, 365-371.
[28]. Hazel, A.; Ross, S. D. *Spectrochim. Acta* **1966**, *22*, 1949-1961.
[29]. Aramendia, M. A.; Borau, V.; Jimenez, C.; Marinas, J. M.; Romero, F. J. *J. Colloid Interface Sci.* **1999**, *217*, 288-298.
[30]. Hirai, H.; Masui, T.; Imanaka, N.; Adachi, G. *J. Alloy and Comp.* **2004,** *374*, 84-88.
[31]. Guo, Y.; Woznicki, P.; Barkatt, A. *J. Mater. Res.* **1996**, *11(3)*, 639-648.
[32]. Nazaraly, M.; Chaneac, C.; Ribot, F.; Wallez, G.; Quarton, M.; Jolivet, J. *J. Phys. Chem. Solids* **2007**, *68(5-6)*, 795-798.
[33]. Von, I. L.; Botto, E. J.; Baran, Z. *Anorg. Allg. Chem.* **1977**, *430*, 283-288.
[34]. Caswell, K. K.; Christopher, M. B.; Murphy, J. C. *Nano Lett.* **2003**, *3(5)*, 667-669.
[35]. Jia, C. J.; Sun, L. D.; Yan, Z. G.; You, L. P.; Luo, F.; Han. X. D.; Pang, Y. C.; Zhang, Z.; Yan. C. H. *Angew. Chem. Int. Ed.* **2005**, *44*, 4328-4333.
[36]. Bao, J.; Zang, R.; Yu. J.; Yang, X.; Wang, D.; Deng, J.; Chen, J.; Xing, X. *Cryst. Eng. Comm.* **2009**, *11*, 1630-1634.